# Single-nucleus RNA sequencing of striatal microglia reveals distinct transcriptomic signatures of acute stress and chronic exercise

Meghan G. Connolly[a], Zachary V. Johnson[c]*, Lynna Chu[d]*, Nicholas D. Johnson[e], Trevor J. Buhr[f,g], Elizabeth M. McNeill[f]*, Peter J. Clark[f,g]*, and Justin S. Rhodes[a,b]*

[a]University of Illinois Urbana-Champaign, Neuroscience Program, Urbana, IL, 61801, USA
[b]University of Illinois Urbana-Champaign, Department of Psychology, Champaign, IL, 61820, USA
[c]Emory University, Department of Psychiatry and Behavioral Sciences, Atlanta, GA, 30322, USA
[d]Iowa State University, Department of Statistics, Ames, IA, 50011, USA
[e]Independent Researcher, USA
[f]Iowa State University, Department of Food Science and Human Nutrition, Ames, IA, 50011 USA
[g]Iowa State University, Neuroscience Graduate Program, Ames, IA, 50011, USA

*These authors contributed equally to this work

**Emails:** meghanc6@illinois.edu, zachary.vernon.johnson@emory.edu, lchu@iastate.edu, johnsonn573@gmail.com, tjbuhr@iastate.edu, emcneill@iastate.edu, pjclark@iastate.edu, jrhodes@illinois.edu

**Corresponding author:**
Meghan G. Connolly
University of Illinois Urbana-Champaign
Neuroscience Program
405 North Mathews Avenue
Urbana, IL 61801
Email: meghanc6@illinois.edu

**Word Count:** 8,040

**Abstract**

Severe acute stress can produce long lasting decreases in voluntary physical activity that contribute to degraded mental and physical health. Stress also produces enduring molecular changes in the striatum, a brain region that regulates voluntary wheel-running and other motivated behaviors. Microglia, the primary immune cells of the central nervous system, have specialized functions in responding to stress, sensing changes in the striatum, and controlling neuronal activity. Thus, microglia are positioned at the interface between neural responses to stress and neural coordination of voluntary activity; however, the role of striatal microglia in stress-induced long-term suppression of voluntary activity remains unexplored. The present study employs single nucleus RNA-sequencing to investigate how stress and exercise impact the biology of microglia in the striatum. We find that stress-induced decreases in running behavior are associated with specific microglial activation profiles. Furthermore, we show that access to a running wheel is associated with an additional and distinct profile of microglia activation characterized by upregulation of complement components and phagocytosis pathways. Lastly, we find that distinct microglial gene sets are associated with general running (versus not running) and more subtle variation in genes with individual running levels. Taken together, our results contribute to a broader understanding of the diverse states that striatal microglia can assume in response to stress and exercise, and broadly suggest that microglia exhibit more nuanced functional responses to environmental perturbations than previously thought.

**Keywords:** Single nucleus RNA-sequencing, exercise, acute stress, microglia, inflammation, motivation, striatum, single cell

## 1. Introduction

A severely stressful event can have long lasting consequences for mental and physical health[1,2]. In humans, traumatic experiences can precipitate depressive-like behavior including decreased motivation for natural rewards and decreased voluntary physical activity[3,4]. Keeping physically active is crucial for maintaining physical and mental health and is considered one of the best ways of coping with stress[5,6]. A better understanding of how an acute episode of severe stress reduces voluntary physical activity will be necessary to develop therapeutic strategies for mitigating the devastating long-term health consequences of traumatically stressful events.

One well-characterized rodent stress model that causes many depressive-like symptoms and results in a prolonged reduction in voluntary locomotor activity is the inescapable shock model[7,8]. Studies have shown that when rodents are exposed to one session of inescapable shock, it reduces their motivation for voluntary wheel running behavior up to 28 days after the stressor[7,8]. Rodents have a natural inclination to run, and rats will lever press for access to a running wheel indicating they find wheel running to be rewarding[9–12]. Thus, the prolonged decreased voluntary running observed in the inescapable shock model is interpreted as a decrease in motivation for or pleasure from running.

Multiple regions of the brain contribute to motivation for voluntary physical activity[13]. The striatum, both its dorsal and ventral areas, is particularly notable for its dual role in motivating reward-seeking behaviors and regulating movement[14–18]. A recent study found major transcriptomic changes in this region in mice that were selectively bred for increased voluntary wheel running behavior[19]. The striatum is also well known to be sensitive to stress, with several studies showing stress altering striatal-dependent behaviors like motivation, locomotion, and associative learning[20,21]. Furthermore, stress also alters the striatum at the cellular and molecular

levels with studies showing that stress alters striatal circuitry[20] and alters striatal secretion of serotonin and dopamine[22]. Given that the striatum is both sensitive to stress and is responsible for integrating emotional information in decision making[18], stress-induced alterations in the striatum may underlie stress-associated decreases in motivation for voluntary physical activity. However, the specific molecular changes in the striatum that persist long after an acute stressor remain unknown, and the key cell types in the striatum involved in the stress-induced suppression of voluntary physical activity remain unexplored.

Microglia are primely positioned to regulate stress-induced suppression of physical activity owing to their roles in neuroinflammation and homeostatic regulation. In response to an acute stressor like inescapable shock, microglia enact a robust but brief neuroinflammatory response[23–25] that subsides within approximately 48 hours. However, microglia can remain in a "primed" state for several weeks after exposure to a stressor [26–30]. This primed state of microglia is distinctively marked by increased baseline levels of inflammation markers and inflammatory mediators, a reduced threshold for activation into a pro-inflammatory state, and an intensified inflammatory response upon activation [26,28,30,31]. In addition to their traditional role as mediators of inflammation, microglia are increasingly recognized for their specialized functions in regulating the extracellular microenvironment in a way that is conducive for brain-region specific signaling[32]. For instance, recent research has highlighted how striatal microglia detect and react to neuronal ATP release by adjusting adenosine levels, thereby helping to maintain striatal homeostasis[33]. Dysregulation of this feedback loop could contribute to altered striatal function and subsequent motivational deficits. However, the specific molecular profile of microglia long after an acute stressor that occurs in coincidence with prolonged reduced voluntary physical activity has not been characterized to our knowledge.

In contrast to the negative impact of stressors on microglia activation and subsequent motivational changes, engaging in physical exercise has been shown to exert positive effects on these crucial immune cells within the central nervous system across the lifespan [34–37]. Regular physical activity has been found to modulate microglial function, promoting an anti-inflammatory phenotype, and enhancing their ability to support the brain in both health and disease [34,38–42]. Studies have demonstrated that exercise induces changes in microglial morphology and gene expression, leading to a more vigilant and protective state [36,38]. This neuroprotective role of physical exercise extends beyond the immediate activation period, with evidence suggesting that regular activity contributes to a resilient microglial profile, reducing the likelihood of priming and exaggerated inflammatory responses to future stressors [43–45]. However, how microglia in the striatum respond to exercise has yet to be elucidated as most of the studies mentioned above focused on other regions of the brain.

The present study used single nucleus RNA-sequencing to investigate how striatal microglia respond to a traumatic acute stressor that causes prolonged decreased motivation for physical activity and voluntary wheel running behavior. To evaluate microglial signatures of stress and exercise, male rats were given one session of inescapable shock stress and then allowed access to a running wheel for 42 days (with the respective controls described below). We predicted that microglia in the striatum of acutely stressed rats would show distinct forms of neuroinflammatory activation, and that physical activity would promote an anti-inflammatory microglial phenotype. Our work deepens our understanding of microglial functional complexity and uncovers candidate molecular and cellular mechanisms underlying stress-associated decreases in motivation for physical activity.

## 2. Materials and Methods

### *2.1 Subjects*

Adult male Sprague Dawley (SD) rats, weighing 250-280g upon arrival to the Iowa State University Vivarium, were chosen per previous work documenting stress-induced long-term wheel running deficits[7,8]. Chow (ENVIGO, Tekland 2014) and water were provided *ad libitum* throughout the experiment. Rooms were controlled for temperature (21 ± 1°C) and photoperiod (12:12 light/dark) for the entire study. All procedures were approved by the Iowa State University Institutional Animal Care and Use Committee and adhered to NIH guidelines.

### *2.2 Experimental Design*

Upon arrival, rats were individually housed in a standard laboratory cage with (Runner) or without (Sedentary) a locked 13-inch diameter running wheel (STARR Life Sciences, PA, USA) for one week. Half of the rats in each exercise condition were then randomly assigned to receive a single episode of 0 (No stress) or 100 (Stress) uncontrollable tail shocks. The tail shock paradigm used in the present study followed our previous publications[22,46,47]. Approximately 2-5 h into the light cycle, rats assigned to the stress condition were restrained in flat bottom Plexiglas tubes with the tail protruding from the back where electrodes were placed to deliver 100, 1.25mA average current, 5-s tail shocks on a variable 1 min inter-shock interval. This procedure lasted approximately 100 minutes, though the precise time varied[22,46,47]. Rats that did not receive stress (i.e. 0 shocks) remained undisturbed in home cages in a different room during the tail shocks.

Forty-eight hours later, running wheels were unlocked and rats were allowed to run freely for the 42-day duration of the study. The 48-hour delay between tail shocks and wheel access was done to minimize the possible development of an association between tail shock exposure and free access to running wheels. Wheel running distance was collected every hour for the

entire 6-week duration of the experiment. This time period was chosen because six, but not three-, weeks of running wheel access can prevent the development of striatum-involved anxiety- and depression-like behavior in rats[48–50]. Moreover, SD rats continue to display acute stress-induced persistent reductions in voluntary wheel running behavior beyond six weeks[7,8]. On Day 42 of wheel access, sedentary and runner rats were euthanized by rapid decapitation during the peak running activity (between 1-5 hours into the dark cycle). The final groups and sample sizes were Sedentary No Stress (n=6), Sedentary Stress (n=6), Runner No Stress (n=6), and Runner Stress (n=6).

In addition to measuring wheel revolutions continuously in 1-hour intervals in the rats that had access to running wheels throughout the entire experiment, we also measured body mass at the beginning and end of the experiment. We measured food consumption on days 21, 23, 25, 27, and 41 by subtracting the total weight of the food pellets in each cage from the prior day's weight. These outcomes were measured to investigate whether stress caused long-term hypophagia. The wheel running data were analyzed using a repeated-measures ANOVA with day as the within-subjects factor and treatment group (stress or no stress) as the between-subjects factor. The differences in body mass between the last day of the experiment and the first day were analyzed using a 2x2 ANOVA, with stress, exercise, and their interaction as factors. The food consumption data were analyzed using a 2x2 repeated-measures ANOVA with the 5 sampling days as the within-subjects factor. When interactions were significant, pairwise differences between means were evaluated using least-significant difference tests.

### *2.3 Nuclei Isolation, Library Construction, and Sequencing*

Rat brains were rapidly extracted. The striatum was microdissected on a glass plate over ice per our previous publications[46,51,52]. The striatum was placed in pre-weighed cryovials, flash-

frozen with liquid nitrogen, and then stored at −80°C until nuclei isolation. For nuclei isolation, the striata from all six animals within each treatment group (i.e. No Stress Sedentary, No Stress Runner, Stress Sedentary, or Stress Runner) were pooled together and placed in a centrifuge tube, lysed, and dissociated together to yield four samples. The nuclei were extracted and counted following protocols described previously[53]. Briefly, frozen striatal tissue was placed in lysis buffer (10 mM Tris-HCL, 10 mM NaCl, 3 mM $MgCl_2$, 0.1% Nonidet P40 Substitute) on ice for 30 min to lyse tissue followed by addition of Hibernate AB complete media (2% B27 and 0.05mM Glutamax, BrainBits HAB-500) and homogenization using a hand-held electronic homogenizer. Pooled homogenates were then centrifuged for 5 min at 600 x g and 4°C. The supernatant was discarded, and sample pellets were washed, resuspended, and then strained twice with 40uM strainers to remove any clumped cells or debris. The nuclei were then stained with 4',6-diamidino-2-phenylindole (DAPI) and flowed through a fluorescence activated cell sorter (FACS) (BD FACSCanto, BD Biosciences, Franklin Lakes, NJ, USA) to assess viability. The nuclei were sorted according to their expression of DAPI and roughly 400,000 viable nuclei were collected per group. Following successful collection of the nuclei, the samples were given to the Iowa State DNA Facility who were responsible for making cDNA libraries using the 10x Chromium kit (3' RNA library prep) (10X Genomics, Pleasanton, CA, USA), and subsequent sequencing on an S1 lane using the NovaSeq 6000 (Illumina, San Diego, CA, USA).

***2.4 snRNAseq Data Analysis***

After sequencing, Raw FASTQ files were aligned to the *Rattus norvegicus* genome using the CellRanger pipeline (10X Genomics, Pleasanton, CA, USA). In total, 900,107,250 reads were sequenced from an estimated 44,629 nuclei. Across pools, the median number of Unique Molecular Identifiers (UMIs) sampled per nucleus ranged from 1,877-2,197, and the median

number of genes sampled per nucleus ranged from 1,200-1,336. Filtered feature matrices generated by CellRanger were further pre-processed to 1) minimize risk of analyzing dead or dying nuclei by excluding barcodes associated with extremely few RNA molecules (<750) and genes (<500), 2) minimize risk of analyzing multiplets by excluding barcodes associated with an extremely large number of RNA molecules (>20,000) and genes (>5,000) suggesting multiple nuclei were sampled in the same droplet, 3) excluding barcodes associated with extremely high mitochondrial gene content (>5% of all genes). Individual rats were recovered from each pooled sample using the demultiplexing algorithm Souporcell[54]. Souporcell operates without the need for a reference genome for each individual by identifying putative individual-specific single-nucleotide polymorphisms (SNPs) associated with droplet-specific barcodes, and then using these SNPs to separate barcodes predicted to come from distinct individuals. Additionally, Souporcell uses these SNPs to estimate a probability that each droplet-associated barcode reflects multiple nuclei derived from genetically distinct individuals. As an additional quality control measure, we excluded those barcodes that were predicted by Souporcell to come from multiple individuals.

### *2.5 Clustering and Isolation of Microglia Cluster*

A data-driven clustering approach was used to dimensionally reduce the data and assign cells to communities based on transcriptomic similarity in R using Seurat [55]. First, we normalized the data and identified variable genes using the 'SCTransform' function from the sctransform package in R. For dimensionality reduction, we performed Principal Components Analysis using the 'RunPCA' function (with dim=50) and Uniform Manifold Approximation (UMAP) using the 'RunUMAP' function to allow for non-linear dimension reduction (dims=1:50, min.dist=0.5, spread=0.2, n.neighbors=50, n.epochs=1000, metric="euclidean"); both functions can be found

in the Seurat package. Lastly, nearest neighbors were identified using the 'FindNeighbors' function (reduction="pca", k.param=50, dims=1:50, n.trees=500, prune.SNN=0) and clusters were assigned using the 'FindClusters' function (resolution=0.2, algorithm=2) for Seurat.

This pipeline resulted in 17 clusters. To aid in cluster identification, each parent cluster was assigned a number (0-16) which can be visualized in UMAP space (**Fig. 2A**). The microglia cluster was identified using genes specific to microglia (*P2ry12*, *Aif1*, *Itgam*, and *Cx3cr1*; see **Fig. 2B**) and the data for this was re-clustered using a similar workflow as above. Since the number of sub-clusters within the microglia cluster was not known *a priori*, this number of clusters was estimated using a non-parametric graph-based approach[56]. The approach involves constructing a k-minimum spanning tree (K-MST), which embeds cells into a similarity graph structure such that an edge exists between cells if they have similar gene expression information. Since different cluster resolutions will lead to different cell clustering assignments, we aim to provide an estimate for the number of clusters that achieves the most separation of cell clusters across different resolutions. To achieve this, the standardized within-cluster edge-count is calculated for a grid of resolution values. Cluster resolutions that result in well-separated cell communities will lead to larger within-cluster edge-counts. It follows that the number of clusters is estimated as the resolution that maximizes the within-cluster edge-count. This graph-based approach circumvents the curse-of-dimensionality that is common in distance-based approaches to estimate the number of clusters, such as the gap statistic[57].

### *2.6 Differential Gene Expression*

For the microglia cluster, gene expression was compared between treatment groups and as a function of running distance using a negative binomial mixed effects model to accommodate correlation between individual rats. This was implemented using the 'glmer' package in R. The

response variable was the number of transcripts of a gene per nucleus. Group (categorical variable) or running distance (continuous variable) was specified as a fixed effect and individual as a random effect. Dispersions were estimated using a Gamma-Poisson model within the 'glmGamPoi' R package[58]. The natural logarithm of the library sizes per nucleus was entered as an offset term to normalize variation in sequencing depth across the nuclei. To correct for multiple testing, we defined significance with an FDR cutoff of 0.05 using Storey's q-value ($q<0.05$)[59]. To determine differentially expressed genes between specific subclusters, the Wilcoxon Rank-Sum approach, which requires no distributional assumptions, was used within Seurat's 'FindMarkers' function.

### *2.7 Gene Ontology*

To test for overrepresentation of biological processes in differentially expressed genes (DEGs), we used the clusterProfiler package in R [60,61]. GO terms were considered significant by Fisher's Exact Test if FDR-corrected $p < 0.05$. In the dot plots generated, GeneRatio is the ratio of input genes that are annotated in a term, count is the number of genes that belong to a given gene set, and the activated versus suppressed pathways are based on the normalized enrichment score (NES). NES is an indicator of the degree of enrichment. A positive NES indicates that members of the gene set tend to appear disproportionately at the top of a ranked input gene list, supporting pathway activation, and a negative NES indicates the opposite circumstance indicating pathway suppression [60,61].

### *2.8 Cellular maturity*

To determine the relative cellular age of microglia clusters, CytoTRACE (Cellular (Cyto) Trajectory Reconstruction Analysis using gene Counts and Expression) was used[62]. CytoTRACE is an algorithm designed to predict the differentiation states of cells based on single-cell RNA

sequencing data. The core principle of CytoTRACE is that less differentiated (immature) cells exhibit higher transcriptional diversity, whereas more differentiated (mature) cells show more specific and lower transcriptional activity. The algorithm operates through several key steps: it begins by normalizing the gene count matrix obtained from single-cell RNA sequencing data to ensure that variations in sequencing depth across cells do not bias the results. It then identifies genes with high variability across the cell population, as these are indicative of differentiation status. For each cell, CytoTRACE calculates a measure of transcriptional diversity, which involves computing the number of unique genes expressed and the expression levels of those genes[62]. Based on this transcriptional diversity, CytoTRACE assigns a score between 0 and 1 to each cell, with a score of 1 indicating a highly immature cell with broad gene expression and a score of 0 indicating a fully mature cell with more specialized gene expression patterns[62]. The CytoTRACE scores for the microglia were then analyzed using a linear mixed model, where the cluster (or sub-cluster) was treated as the fixed effect and the individual samples were treated as the random effect. This statistical approach allows for the evaluation of cluster-specific effects while accounting for variability between individual samples, helping to identify differentiation states across the clusters while controlling for potential confounding factors related to individual differences.

### *2.9 Nuclei Proportions*

The proportion of nuclei distributed within microglia sub-clusters between all groups was determined and was tested for significant differences using a Chi-square test and Fisher's Exact Test for pairwise comparisons. For group differences, we used a significance threshold of alpha=0.05.

## 3. Results

### *3.1 Acute stress persistently impairs running behavior*

The control rats that had access to running wheels (not stressed) ran typical levels for Sprague Dawley males with increasing distance over time[63–65]. Analyses of running distance over the course of the experiment (42 days) showed that stressed rats ran a significantly shorter distance than rats that were not stressed. This was supported by a significant main effect of stress in an analysis of running distance across days ($F(1, 10)=24.4$, $p<0.001$). Rats tended to run farther each day, as indicated by a main effect of day ($F(41, 410)=10.4$, $p<0.001$). The difference in running distance between stressed and non-stressed animals increased across the days (stress x day interaction, ($F(41, 410)=6.5$, $p<0.0001$). Collapsed across days, stressed animals ran 14.9% of the amount that non-stressed animals ran (**Fig. 1B**). Results for body mass and food intake for all rats are reported in Supplementary Results and shown in **Supplementary Figure 1A-B**.

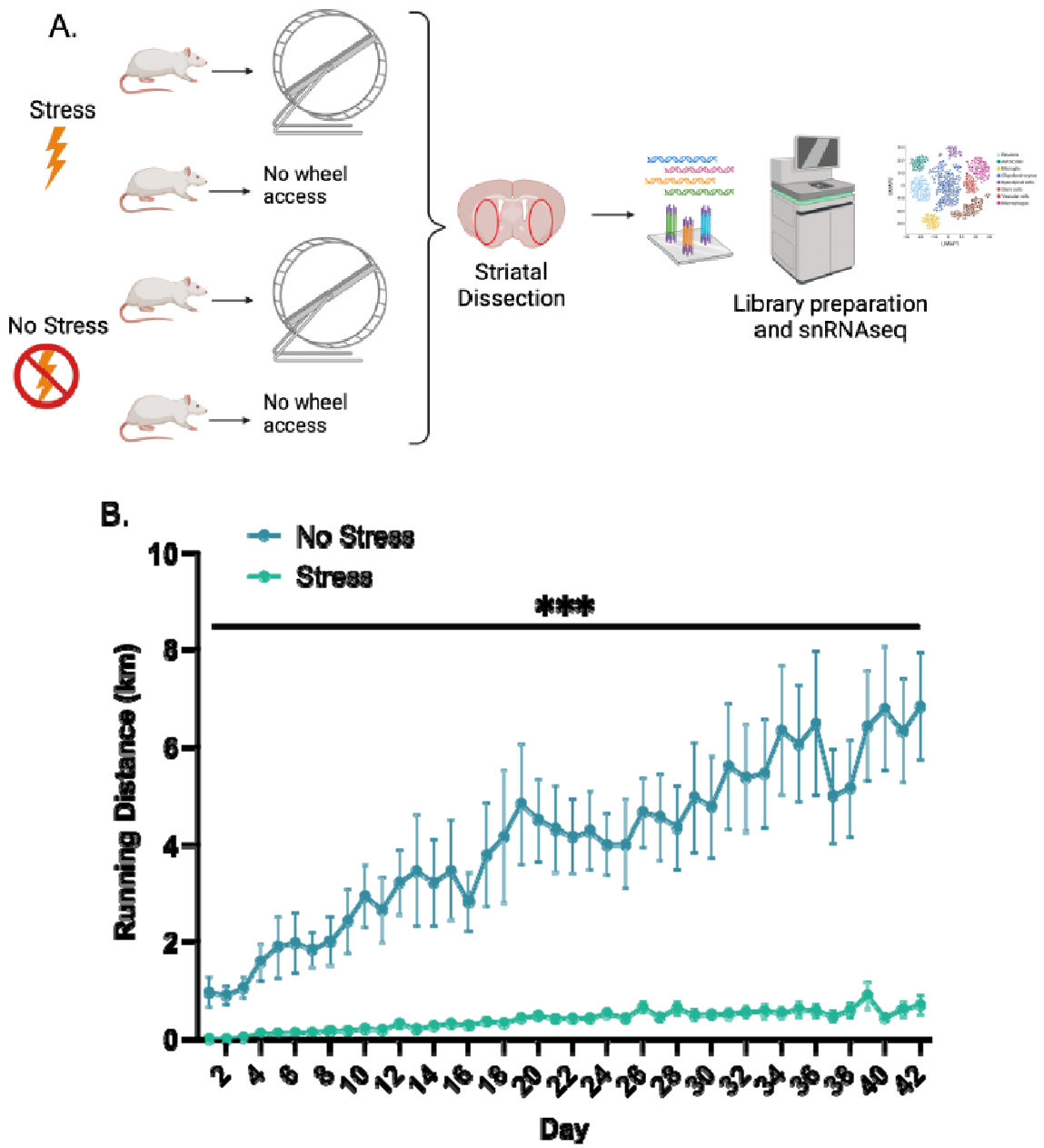


**Figure 1. Persistent psychological effect of acute stress is visible up to 42 days after the stressor as substantially depressed voluntary wheel running behavior.** (**A**) Rats were split into four groups (n=6 per group) that received either one bout of inescapable stress or not and were then given access to a running wheel or not. The striatum was removed and used for single-nucleus RNA-sequencing (snRNAseq) (created with BioRender.com). (**B**) Stressed rats ran significantly less than non-stressed rats over the entire 42-day period (marked by ***; $p<0.001$).

### *3.2 Identification of microglia clusters*

The clustering algorithm identified a total of 17 parent clusters based on the cellularly resolved transcriptomes (**Fig. 2A**). To determine which cluster(s) were microglia, the expression of several genes that are considered markers of microglia (*P2ry12*, *Aif1*, *Itgam*, and *Cx3cr1*) was plotted using the 'FeaturePlot' function in Seurat. This function colors single nuclei on a dimensional reduction plot if they express the marker gene (**Fig. 2B**). All four genes were expressed in parent clusters 2, 13, and 14 so a Dot Plot of more microglia-specific genes (*P2ry12, P2ry13, Cd83, C1qa, Trem2, Aif1, Itgam, Plxdc2, Cx3cr1, Tmem119, Slc2a5, Fcer1g, Sirpa, Selplg, Gpr84, Spi1, Sall1, Hexb, Cst3, Csf1r, Pros1, Slco2b1, Mrc2*) as well as macrophage-specific genes (*Msr1, Clec4e, Slfn4, Itgal, Ptprc, Adgre1, Mrc1, Cd44, Siglec1, Cd274, Fcgr1a, Cd68, Ms4a7, Pf4, F13a1*) was made to examine the difference between the clusters (**Fig. 2C**). Cluster 13 showed strong expression of more macrophage-specific genes while clusters 2 and 14 showed strong expression of microglia-specific genes (**Fig. 2C**). Thus, we considered clusters 2 and 14 as containing nuclei from microglia. To understand the difference between the two microglia clusters, CytoTRACE was employed to see if there was a relative difference in cell age. As stated above (in methods section 2.8), CytoTRACE assigns a differentiation score to each cell based on transcriptional diversity, with higher scores indicating less differentiated cells. This allowed us to compare the differentiation states between the two clusters effectively. Cluster 14 showed a significantly greater CytoTRACE score compared to cluster 2 ($\beta = .47$, SE= .013, $p<.0001$) suggesting that cluster 14 consists of relatively immature microglia while cluster 2 consists of relatively mature microglia (**Fig. 2D**) (**Supp. Table 1**).

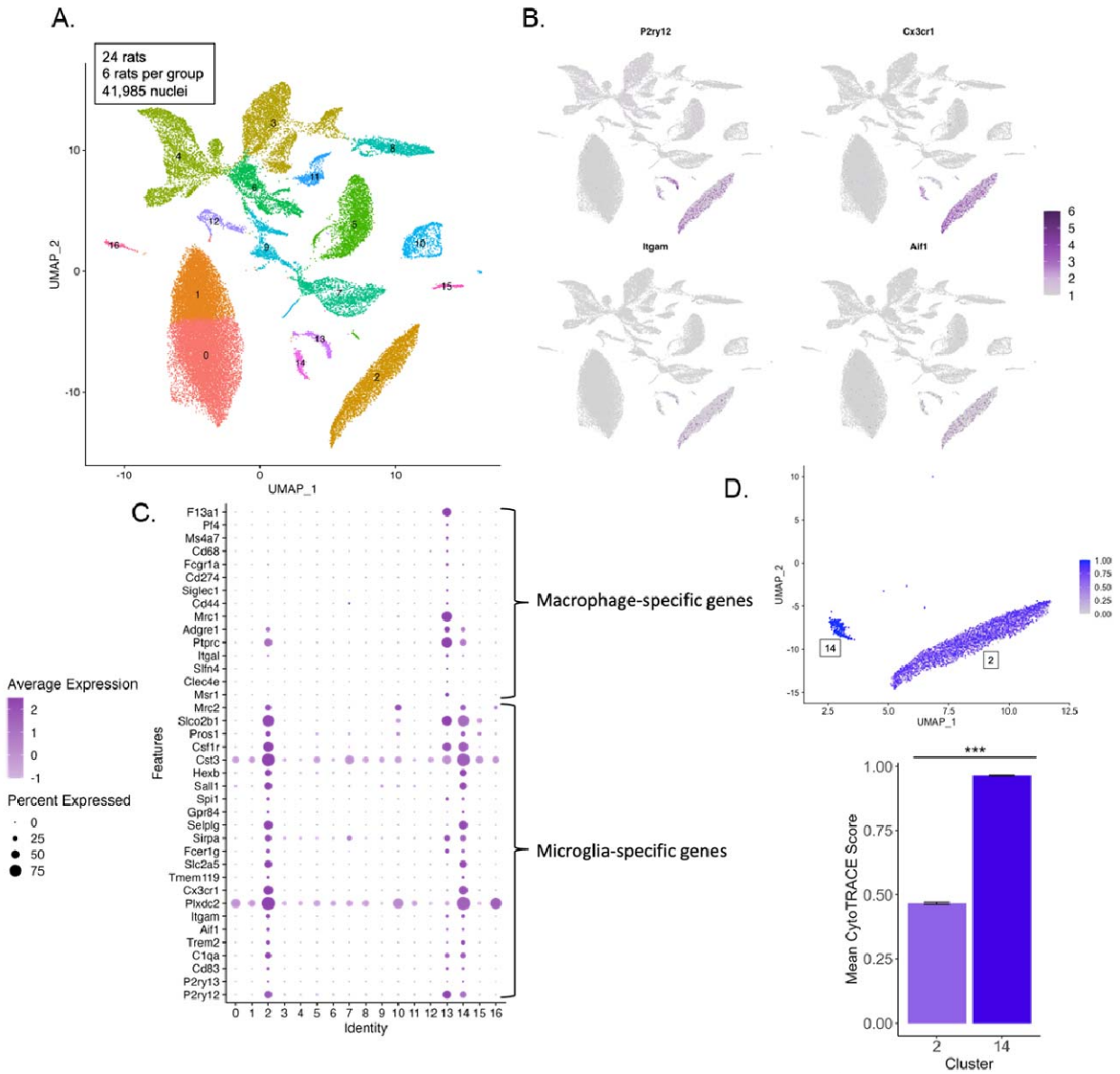


**Figure 2. Microglia clusters revealed through analysis of canonical markers and cellular maturity.** (**A**) The 41,985 total nuclei from cells in the striatum were split into 17 distinct clusters based on their transcriptomes. (**B**) UMAP plots showing expression of key microglia-related genes identified clusters 2, 13, and 14. (**C**) To distinguish between these three clusters, the percentage of cells and average expression of microglia-specific and macrophage-specific genes on a dot plot showed that clusters 2 & 14 are microglia, while cluster 13 are macrophages. (**D**) The difference between the microglia in clusters 2 & 14 was determined using CytoTRACE

which showed that cluster 14 is composed almost exclusively of relatively immature microglia, while cluster 2 (containing a total of 3,859 nuclei) contained a more diverse composition of intermediate maturity scores (marked by ***; $p<0.001$). The bars represent means of all the nuclei collapsed across all individuals, and standard errors refer to variation among nuclei not individuals.

### *3.3 Striatal microglia signatures of stress*

To investigate signatures of stress in striatal microglia, we first compared gene expression within the relatively mature microglia cluster (i.e., cluster 2) between the non-stressed sedentary group (no stress control) and the stressed sedentary group (six-weeks post-stressor exposure, but when behavioral impacts are still apparent, **Fig. 1B**). We found 24 differentially expressed genes (stress-DEGs), of which 3 were upregulated in the non-stressed animals while the remaining 21 were upregulated in the stressed animals (**Fig. 3A**) (**Supp. Table 2**). A chi-square goodness-of-fit test revealed this distribution of 3 to 21 was significantly different from 50:50, i.e., significantly more genes were upregulated in the stress group than vice versa ($\chi_1^2$= 13.5, $p < 0.001$). Several stress-DEGs that were upregulated in the stress group have previously been shown to reflect microglia activation, including *Cst3*, *Apoe*, *C1qa*, and *C1qb* [66–71] (**Fig. 3B**).

To further evaluate differences between the non-stressed and stressed animals, we re-clustered parent cluster 2 (i.e., relatively mature microglia cluster) and found three distinct sub-clusters (**Fig. 3C**). CytoTRACE analysis showed the sub-clustering divided the cells based on relative level of cellular maturity. The most immature subcluster was 0, followed by 2, then 1 (**Fig. 3D**) (**Supp. Table 3**). Thus, for the sake of clarity, hereafter, we refer to these subclusters as immature, intermediate, and mature, rather than 0, 2, and 1 respectively.

Stressed animals displayed greater relative proportions of mature microglia and a lesser relative proportion of immature microglia compared to the no stress animals ($\chi_2^2$ = 113.88, p < .0001; pairwise differences indicated stress differed from no stress in proportion of immature and mature, p<0.05, but not intermediate cell numbers; **Fig. 3E & 3F**). Within each of the subclusters, we observed only a few stress-DEGs (**Supp. Tables 4, 5, 6**), consistent with stress-associated gene expression patterns observed in parent cluster 2 being driven largely by stress-associated differences in maturity status of microglia. Based on previous work that correlated cell maturity levels with microglia activation-related gene expression, a score was generated for genes involved in glial metabolism, pro-inflammatory activation (M1), and anti-inflammatory activation (M2) (**Supp. Table 12**)[72]. The score was generated by dividing the number of transcripts for each gene of interest by the total transcripts for each nucleus. There was no significant difference between the stress and no stress animals for the scores, nor was there a difference between subclusters (**Supp. Fig. 2A-C**). This suggests that the canonical M1/M2 designations are not found in microglia long after the stressor, and in our study, are not correlated with cell maturity.

Comparison of DEGs between the relatively mature and immature cells (maturation-DEGs) using the Wilcoxon Rank Sum test showed that there were 4,404 total significant DEGs of which only 58 were upregulated in the mature cluster and the remaining 4,346 were upregulated in the immature cluster (**Fig. 3G & 3H**) (**Supp. Table 7**). To further characterize functional differences between the relatively mature and immature subclusters, maturation-DEGs were evaluated for enrichment of specific gene ontology pathways (**Fig. 3I**) (**Supp. Table 19**). Enriched pathways included those related to metabolism, immune system processes, glutamate signaling, and synaptic changes. The results from gene ontology pathways along with gene

expression are consistent with altered synaptic signaling and enhanced metabolic activity in relatively immature microglia.

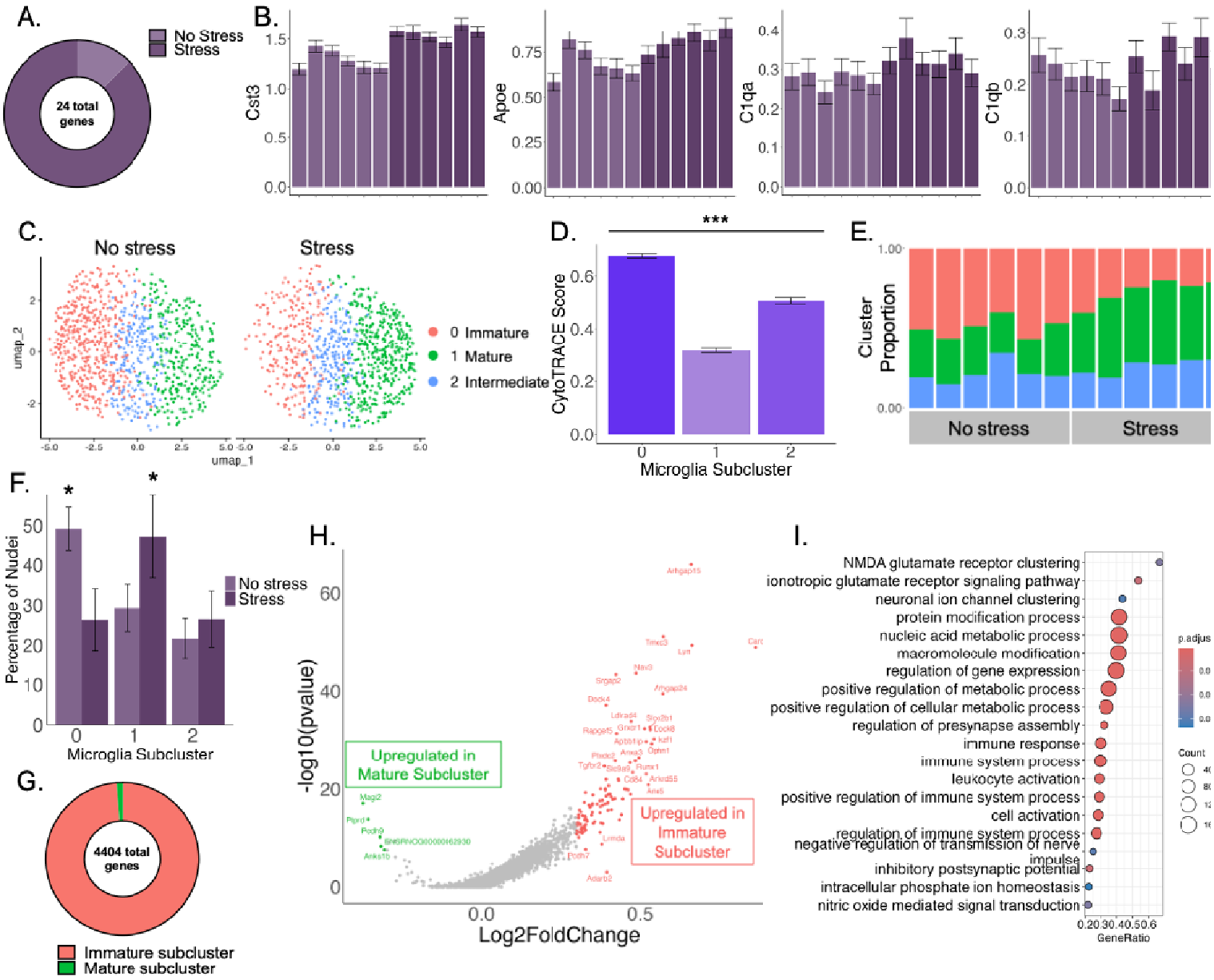


**Figure 3. Acute stress produces prolonged striatal microglia activation.** (**A**) A comparison of gene expression between the no stress and stress groups found a total of 24 differentially expressed genes, or stress-DEGs. The majority of these 24 stress-DEGs were upregulated in the stress group relative to no stress. (**B**) Mean gene expression (SCTransformed) of exemplar genes upregulated in the stress group that are related to microglia activation are shown. Individual

means and standard errors (among nuclei) are shown for all individuals in the no stress and stress groups. (**C**) Re-clustering of microglia showed three subclusters: subcluster 0 (pink), subcluster 1 (green), and subcluster 2 (blue). (**D**) These subclusters could be differentiated based on levels of cellular maturity as measured by CytoTRACE. Hereafter we refer to cluster 0 as the relatively immature cluster, subcluster 2 as intermediate, and cluster 3 as mature. (**E**) Proportions of nuclei in each subcluster are shown for each of the individuals. (**F**) Individuals in the stress group displayed a significantly lower proportion of relatively immature microglia and higher proportion of relatively mature microglia than individuals in the no stress group (marked with *; $p<0.05$). **(G & H**) A comparison of gene expression between the relatively immature and mature subclusters identified 4,404 DEGs, the vast majority of which were upregulated in the immature subcluster, as expected. (**I**) Gene ontology pathways significantly enriched from DEGs between sub-clusters 0 and 1 are shown in the dot plot.

### *3.4 Striatal microglial signatures of exercise enrichment*

We next investigated the effects of exercise enrichment, operationally defined as access to a running wheel (for review, see [73–75]), on the biology of striatal microglia. We first compared the no stress sedentary group to the no stress exercise enrichment group and identified 201 significant differentially expressed genes between sedentary and exercise enrichment groups (exercise enrichment-DEGs), 158 upregulated in the sedentary group and 43 upregulated in the exercise enrichment group (**Fig. 4A**) (**Supp. Table 18**). A chi-square goodness-of-fit test found this distribution of 158 to 48 was different from 50:50 ($\chi_1^2$ = 65.796, $p < 0.001$), indicating exercise enrichment-DEGs tended to be upregulated in the sedentary group. Examples of two genes that were upregulated in the sedentary group and two genes upregulated in the exercise enrichment group are shown in **Figure 4B**. Specific gene ontology pathways that were

significantly over-represented for exercise enrichment-DEGs included: cellular respiration/oxidative phosphorylation, immune response, synaptic signaling, and neurogenesis (**Fig. 4C**) (**Supp. Table 20**). These results are consistent with exercise enrichment shifting striatal microglia toward functions related to synaptic signaling and remodeling via phagocytosis of neuronal processes.

To further analyze the effects of exercise enrichment on microglia, we re-clustered parent cluster 2 with only the exercise enrichment and sedentary no stress groups. This analysis revealed 4 distinct sub-clusters (**Fig. 4D**). As compared to the microglia from sedentary animals, adding the exercise enrichment group revealed a distinct subcluster that was not present when microglia were sub-clustered for sedentary groups alone (as shown above **Fig. 3A**). This subcluster was consistently apparent in all individual runners and nearly absent in all the sedentary individuals (**Fig. 4D**) (**Supp. Fig. 3**). Thus, this subcluster is referred to as the 'exercise enrichment' subcluster hereafter for the sake of clarity. CytoTRACE supported that the remaining three subclusters were distinguished by relative maturity, mirroring the pattern observed in our earlier analyses of stress versus no stress groups, and thus these subclusters are again referred to as the immature, intermediate, and mature. Notably, the exercise enrichment subcluster and the intermediate subcluster displayed similar CytoTRACE scores, supporting they were both composed of relatively intermediate microglia (**Fig. 4E**) (**Supp. Table 8**).

The relative proportions of the four microglial subclusters differed between exercise and control groups ($\chi^2_3$= 157.62, p < .0001) (**Fig. 4F & 4G**). The greatest difference was observed in the exercise enrichment subcluster. In the exercise enrichment group, 14.4% of microglia (in parent cluster 2) belonged to the exercise enrichment subcluster, whereas only 1.9% belonged to this subcluster in sedentary rats. The exercise enrichment group also displayed relatively fewer

intermediate and immature microglia, but relatively more mature microglia compared to sedentary rats (**Fig. 4F & 4G**). The genes upregulated in the exercise enrichment cluster relative to the other subclusters were generally found to be involved in microglia activation/immune response (*Cst3, Marcks, Sparc, Cd83, Dab2, Tmem176a, Tmem176b, Clec4a1, and Cd74*), the complement system (*C1qa, C1qb, C3*), and microglia phagocytosis (*Ctss, Pltp, RT1-DMa*) (**Fig. 4H**). To evaluate the differences between the subclusters, M1, M2, and metabolism scores were again generated as described above (**Supp. Table 12**)[72]. No significant differences between exercise and sedentary groups or between subclusters were observed (**Supp. Fig. 2D-F**), indicating canonical descriptions of microglia activation do not differentiate subtypes of microglia in response to exercise enrichment.

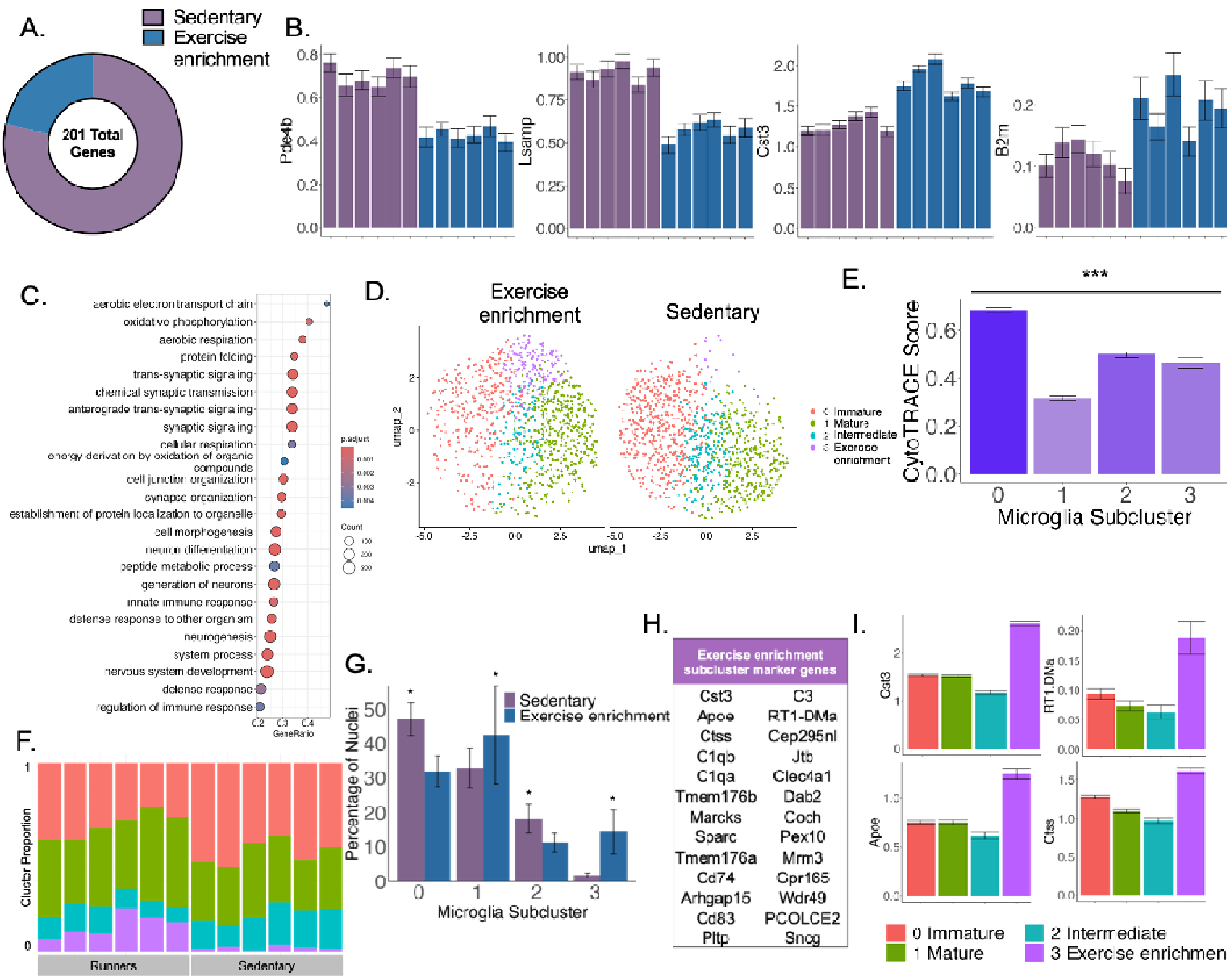


**Figure 4. Enrichment from exercise is associated with a specific striatal microglia activation profile.** (**A**) A comparison of gene expression between the sedentary and exercise-enrichment groups found a total of 201 differentially expressed genes, or exercise enrichment-DEGs. The majority of the 201-exercise enrichment-DEGs were upregulated in the sedentary group relative to the exercise enrichment group (**B**) Mean gene expression of exemplar genes upregulated in the sedentary and exercise enrichment groups are shown. Individual means and standard errors (among nuclei) are shown for all individuals in the sedentary and exercise

enrichment groups. (**C**) Gene ontology pathways significantly enriched from exercise enrichment-DEGs are shown in the dot plot. (**D**) Re-clustering revealed four distinct subclusters of microglia in the sedentary and exercise enrichment groups. (**E**) CytoTRACE analysis revealed a similar maturity structure as the stress vs. no stress analysis (subcluster 0 = immature, subcluster 1 = mature, and subcluster 2 = intermediate), except that a new cluster appeared that did not exist for animals housed without running wheels. Thus, we refer to this new class of microglia as the exercise enrichment subcluster. The exercise enrichment subcluster showed a relative maturity level similar to the intermediate subcluster. (**F**) Proportions of nuclei in each subcluster are shown for each of the individuals. (**G**) Individuals in the exercise enrichment group displayed a significantly lower proportion of relatively immature microglia, and a higher proportion of relatively mature microglia and especially higher proportion of microglia in the exercise enrichment subcluster, which was nearly absent in sedentary rats (marked with *, $p<0.05$). (**H**) Comparison of the exercise enrichment subcluster, which is markedly absent in the sedentary group, to the other subclusters revealed a distinct set of genes involved in activation, phagocytosis, and the complement system. (**I**) Examples of expression of these genes across the four subclusters are shown.

### *3.5 Striatal microglial signatures of individual running levels*

To more deeply investigate the effects of exercise on striatal microglia, we analyzed differential gene expression associated with levels of voluntary wheel running in non-stressed rats across multiple timescales relative to when the animals were sampled: the previous 40 days, the previous day, the previous three hours, the period 30-90 minutes before sampling, and the 30-minute period immediately before sampling (**Supp. Table 9**; **Supp. Tables 13-16, respectively**). Strikingly, there were 807 significant running level-DEGs when the running covariate was the

total distance run over the entire 40-day period, but only 58 DEGs were observed when the running covariate was total distance run during the final 24 hours before collection. Further, when running during the past 3 hours, 30-90 minutes, or 30 minutes was used, even fewer significant DEGs were observed (20, 20, and 9, respectively). All the DEGs found for analyses using 24 hours, 3 hours, 30-90 minutes, or 30 minutes as running covariates were also significant DEGs when the entire 40-day period was used as the running covariate. Individual running levels over the entire 40-day period were correlated with levels of running at the smaller intervals, with decreasing correlations as the intervals became smaller and more proximal to sampling times (Pearson's R was 0.47, 0.14, 0.1, and 0.03 for 24 hours, 3 hours, 30-90 min and 30 min respectively). Taken together, these results indicate that robust changes in striatal microglia gene expression are mostly strongly associated with levels of running over long time periods.

Interestingly, there was little overlap between running level-DEGs and exercise enrichment-DEGs as indicated by hypergeometric test (p=0.66). This implies that different genes are regulated by running levels in microglia as compared to access to a running wheel (**Supp. Fig. 4A**). Examples of the relationship between gene expression and total running distance for several significant genes are shown in **Supplementary Figure 4B**. Together, the data suggest that exercise enrichment-DEGs largely reflect the environmental enrichment of exercise while running level-DEGs reflect responses to chronic running.

### *3.6 Striatal microglial signatures of interactions between stress and exercise*

Next, we analyzed all groups together using a 2x2 design with stress and exercise as main effects as well as a stress by exercise interaction term. We found a total of 207 significant exercise-DEGs (main effect of exercise), 201 stress-DEGs (main effect of stress), and 17 interaction-DEGs (**Supp. Table 10**). Examples of the interaction-DEGs are shown in **Figure 5A**.

The DEG lists for main effects of stress and exercise overlapped significantly with the stress-DEG and exercise enrichment-DEG lists from the analyses described above where stress and exercise were analyzed separately (**Supp. Fig. 5A & 5B**; hypergeometric tests, both $p<0.05$). To explore whether a similar set of genes were altered by both stress and exercise, we compared the DEG lists for exercise and stress (both from the 2x2 model and each factor separately) using the hypergeometric test. No significant overlaps were detected (**Fig. 5B & 5C**). This indicates that stress and exercise are inducing distinct patterns of activation in striatal microglia.

To further analyze microglia across all four groups, we re-clustered parent cluster 2 which yielded three distinct subclusters (**Fig. 5D**). Similar to the analysis of the runners, there was a running specific subcluster (subcluster 2) (**Fig. 5E & Fig. 5F**). Analysis of cell maturity using CytoTRACE showed that subcluster 1 was relatively immature and subclusters 0 and 2 (the runner subcluster) were equally relatively mature (**Fig. 5G**) (**Supp. Table 11**). The proportion of nuclei in each subcluster differed between treatment groups in an overall Chi-square test ($\chi^2_6$= 383.59, $p < 0.0001$). Within each subcluster, all pairwise comparisons between treatment groups were significant as indicated by Fisher exact test (**Fig. 5E**). To determine whether the subclusters might differ in additional biological dimensions, M1, M2, or metabolism scores were generated (**Supp. Table 12**). Relative to the immature subcluster 1, the mature subcluster 0 displayed greater metabolism scores and decreased expression of both M1 and M2 genes, whereas the runner subcluster 2 displayed only decreased expression of the M1 genes (**Fig. 5H**). No significant differences between treatment groups were observed for the M1, M2, or metabolism scores. Taken together, these data suggest the running subcluster displays an M2 phenotype suggesting a protective microglial functional state.

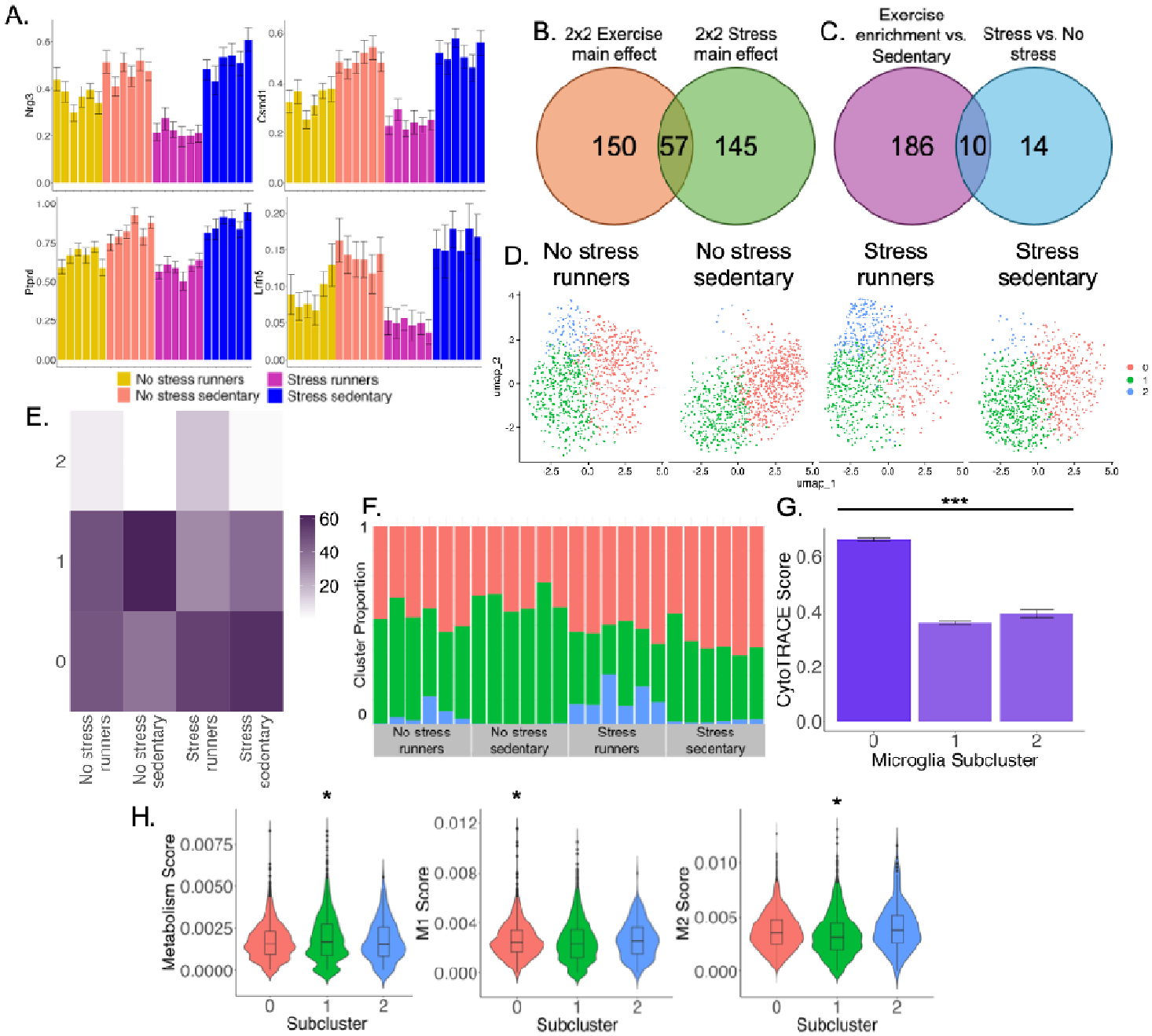


526

527 **Figure 5. Striatal microglia activation signatures of stress-exercise interactions.** (**A**)

528 Analysis of all four groups yielded 207 significant exercise-DEGs (main effect of exercise), 201

529 stress-DEGs (main effect of stress), and 17 interaction-DEGs. Mean normalized gene expression

530 for four exemplar interaction-DEGs are plotted. Individual means and standard errors (among

nuclei) are shown. (**B**) The stress-DEG list and exercise enrichment-DEG list from the main effects of the 2x2 analysis did not significantly overlap. (**C**) Similarly, the stress-DEG and exercise enrichment-DEG lists from the separate analyses did not overlap. (**D**) Re-clustering of microglia from all treatment groups resulted in three distinct subclusters, including a subcluster that is only apparent in runners (subcluster 2). (**E**) Proportions of nuclei in each subcluster are shown for each treatment group. (**F**) The runner subcluster accounted for a large percentage of microglia in all individuals that had access to running wheels (both stress and no stress), regardless of running levels, but was almost entirely absent in individuals without running wheels. (**G**) Subcluster 1 was relatively more immature than the other clusters (marked by ***; $p<0.001$). (**H**) The subclusters were differentiated based on genes related to metabolism, pro- (M1), or anti-inflammatory (M2) activation. Specifically, the runner subcluster showed a lower metabolism score and higher M2 score compared to the relatively mature subcluster 1.

Finally, we ran an analysis of covariance (ANCOVA) to determine how stress and individual running distance might interact to influence gene expression (**Supp. Table 17**). There were 401 significant running level-DEGs, 379 significant stress-DEGs, and 355 significant stress-by-running level interaction DEGs. The DEG list for the correlation between running distance for only the non-stressed runners, and the DEG list for the running covariate in the ANCOVA significantly overlapped ($p < 0.001$) (**Supp. Fig. 5D**). The DEG list from the stress versus no-stress (all sedentary) analysis (**Supp. Table 2**) did not overlap with the DEG list for the main effect of stress in the ANCOVA ($p>0.05$) (**Supp. Fig. 5C**). This result indicates an overall strong exercise-by-stress interaction effect in our data where the effects of stress on striatal microgial gene expression largely depend on whether animals had access to a running wheel or

not. Examples of genes that showed strong effects of the running covariate, a strong effect of stress, and no interaction are shown in **Supplementary Figure 5E & 5F**. Examples of genes that showed a strong interaction between the running covariate and stress are shown in **Supplementary Figure 5G**. Taken together, these results indicate an extraordinary sensitivity represented in the molecular signatures of striatal microglia to complex interactions between stress and exercise.

## 4. Discussion

The central aim of this study was to define the molecular imprints of stress, exercise, and their convergence within striatal microglia. Using snRNA-seq, we uncovered stress-associated differences in estimated microglial maturity 42 days post-stressor as well as molecular signatures of a distinctive and non-canonical activation pattern, underscoring the enduring impacts of stress on microglial dynamics. Access to a running wheel was also associated with profound alterations in striatal microglia, manifesting as greater relative proportions of a distinct subpopulation that was nearly absent in sedentary rats. This subpopulation showed heightened expression of both complement system- and phagocytosis-related pathways, indicative of a separate, distinct form of microglial activation. Even more striking, we observed distinct microglial gene expression signatures associated with access to a running wheel (i.e., exercise enrichment) compared to individual running distances. Lastly, we observed evidence for a distinct form of neuroinflammatory activation in response to both stress and exercise, potentially reflecting molecular processes that contribute to deficits in motivation for physical activity. Our findings thus support a broader spectrum of microglial functional states than previously appreciated and

reveal candidate molecular pathways by which striatal microglia may regulate motivation for exercise following stressors.

In the rats exposed to inescapable foot shocks (i.e., the stress group), there was an enduring behavioral effect that was clearly visible for 42 days after the stressor as indicated by severely depressed levels of voluntary wheel running behavior (**Fig. 1B**). This extends previous literature where reduced voluntary running was observed up to 28 days after the stressor[7,8]. We hypothesized that microglia-induced neuroinflammation and/or priming of microglia in the striatum might contribute to the reduced motivation for running given the role of microglia in both stress and exercise (as reviewed in [31,35]). Consistent with our hypothesis, several genes that have been implicated in microglia activation were upregulated in the stress group: *Cst3, Apoe, Srsf7, Rpl19, C1qa,* and *C1qb* (some of which are plotted in **Fig. 3B**). *Cst3* and *Apoe* were documented previously as markers of activated microglia[66], disease-associated microglia[66,67], or injury-associated microglia[68,69]. In contrast, *Srsf7* and *Rpl19* have been found to be downregulated in microglia in Alzheimer's disease[76] and are associated with homeostatic microglia[77] however, in our study both were upregulated with stress. Both *C1qa* and *C1qb* are involved in the complement system which are indicators of microglia activation as well [70,71].

In addition to displaying differential expression of specific markers of microglia activation as described above, stress was also associated with greater estimated microglial maturity (**Fig. 3D & 3E**), a pattern that may reflect a specific form of inflammatory action. Ruan et al. (2023) used CytoTRACE in their experiment examining the role of leucine-rich alpha-2-glycoprotein 1 (Lrg1) in cerebral ischemia reperfusion injury and similarly found that different clusters of microglia had different states of maturation which they attributed to their inflammatory action. On the other hand, we did not see evidence of canonical markers of stress-

induced inflammation such as *Il1β*, *Il6*, or *Tnfα* even though transcripts for these genes were detected in our dataset. Similarly, while we were able to detect expression of many genes that are considered markers of M1, M2, and metabolism states of microglia, these genes were not informative for distinguishing subclusters or effects of stress in sedentary rats (**Supp. Fig. 1A-F**). Together, this supports a unique form of enduring microglial activation following an acute severe stressor that is not described by canonical markers of microglia activation (i.e., M1 and M2). This is consistent with previous work showing enduring responses of hippocampal and cortical microglia to inescapable shock stress[24,25,28,78]. Given the dual role of inescapable shock stress in producing both microglial activation and reduced motivation for exercise, it is possible that the reduced running we see in the present study is a result of the sustained striatal microglial activation following inescapable shock stress. Future studies are needed to determine if blocking striatal microglia activation ameliorates deficits in motivation for physical activity following exposure to a severe, acute stressor.

In addition to exhibiting molecular signatures of stress, microglia also exhibited molecular signatures of physical activity. Individuals with running wheel access that were not stressed ran every day throughout the experiment, and total running distance was associated with expression levels of 807 genes (**Supp. Table 9**). These effects were unlikely driven by acute effects of running, because more than 10-fold fewer running-level DEGs were observed when analyzing shorter intervals immediately prior to sampling compared to the total distance run over previous 40 days. This supports the idea that the cumulative effect of running over multiple days or weeks results in a robust functional shift in a subset of microglia, perhaps to support striatal function during running behavior.

In addition to running-level DEGs, we also detected a separate set of non-overlapping genes associated with running wheel access (**Supp. Fig. 4A**), supporting distinct microglial profiles associated with running wheel access versus levels of running. Access to a running wheel is considered a form of enrichment [79–81]. Thus, we believe the DEGs identified in the comparison of runners to sedentary rats (no stress) reflect the enrichment of the running wheel, or the deprivation of no running wheel in the sedentary group, rather than differential levels of physical activity *per se*. Strikingly, we observed an 'exercise enrichment' subcluster that is only found in animals with access to a running wheel, whether stressed (and thus, running very low levels) or not (**Fig. 5D-F**). The genes in this subcluster were generally involved in microglial activation/immune response (*Cst3, Marcks, Sparc, Cd83, Dab2, Tmem176a, Tmem176b, Clec4a1, and Cd74*) the complement system (*C1qa, C1qb, C3*), and microglial phagocytosis (*Ctss, Pltp, RT1-DMa*) (**Fig. 4D**). Together, these genes support the idea that microglia are activated and phagocytosing in a complement-dependent manner more in rats with voluntary wheel running enrichment than those deprived of the enrichment.

Activated microglia can eliminate both damaged cells and dysfunctional synapses, a phenomenon known as "synaptic stripping" [70,82–85]. C1q and C3, integral components of the classical complement cascade, attach to the surface of invading pathogens. Subsequently, phagocytes expressing target complement receptors in the peripheral immune system eliminate these pathogens [86,87]. Similarly, within the CNS, microglia utilize classical complement cascades to facilitate phagocytic signaling, leading to the removal of excess synapses [70,71]. Few studies have evaluated microglial complement and phagocytosis during physical exercise, but persistent aerobic exercise has the potential to preserve the integrity and functionality of neurovascular units in aging mice[88]. This is achieved by diminishing C1q-positive microglia and enhancing

neuroplasticity [88]. Moreover, physical exercise appears to facilitate cellular communication between microglia and neurons through complement molecules [89]. Thus, the emergence of a unique C1q+ and C3+ microglial subpopulation with exercise may be involved in neuron-microglia and/or astrocyte-microglia crosstalk.

In addition to uncovering striatal microglia signatures of traumatic stress and separately, voluntary wheel running, we were also interested in exploring potential interactions of running and stress on microglia. When examining the effects of stress and running on gene expression using an ANCOVA, the stress-DEGs did not significantly overlap with the stress-DEGs in rats housed without running wheels (**Supp. Fig. 5C**); however, a suite of eight genes (*Apoe, C1qa, Cst3, Grm3, Mt.co1, Pde4b, Rpl19,* and *Tmem176b*) was differentially expressed in response to both stress and exercise. Notably, these genes are almost all involved in microglia activation (**Supp. Fig. 6**). Based on these data, we hypothesize that microglia are generally activated but exhibit different subtypes of responses to stress depending on exercise enrichment; however, future studies are needed to test this hypothesis.

We investigated microglial metabolism, pro-inflammatory activation (M1), and anti-inflammatory activation (M2) by tracking established transcriptional markers of these functional states. When all four experimental groups were analyzed together in a 2x2 design, microglia clustered into three subclusters, the exercise enrichment subcluster (more abundant in runners regardless of stress condition), relatively mature cluster (more abundant in stressed versus non-stressed rats), and relatively immature cluster. The exercise enrichment subcluster showed an increased M2 score compared to the relatively mature subcluster (**Fig. 5E**), further supporting distinct microglia signatures of stress and exercise, with exercise promoting shifts toward anti-inflammatory activation.

In conclusion, this study demonstrates the enduring impact of a single traumatic stressor on voluntary wheel running and striatal microglial activation. Further, we establish that striatal microglia display distinct molecular signatures of activation in response to stress versus exercise. Notably, the observed signature of microglia activation following acute stress, coupled with the emergence of a unique exercise-induced subcluster associated with activation and phagocytosis, underscores the complex and multidimensional nature of microglial responses. The exercise enrichment subcluster further supports that microglial functional diversity extends beyond traditional M1 and M2 categories. The specific signature of changes in activation 42 days post-stress also highlights the temporal complexities of microglial responses and has potential implications for long-term priming. Future research should further investigate microglial functional diversity and causally manipulate striatal microglia to determine their functional role in modulating motivational deficits associated with stress.

**CRediT Author Contributions:**

**Meghan G. Connolly:** Conceptualization, Methodology, Formal Analysis, Software, Investigation, Writing – Original Draft, Writing – Review & Editing, Visualization, Project Administration. **Zachary V. Johnson:** Methodology, Formal Analysis, Software, Investigation, Data Curation, Writing – Review & Editing. **Lynna Chu:** Methodology, Formal Analysis, Software, Investigation, Data Curation, Writing – Review & Editing. **Nicholas D. Johnson:** Methodology, Formal Analysis, Software, Writing – Review & Editing. **Trevor J. Buhr:** Investigation. **Elizabeth M. McNeill:** Resources, Methodology. **Peter J. Clark:** Conceptualization, Investigation, Methodology, Resources, Writing – Review & Editing,

Funding Acquisition. **Justin S. Rhodes:** Conceptualization, Methodology, Formal Analysis, Software, Investigation, Writing – Original Draft, Writing – Review & Editing, Supervision.

**Conflict of Interest:**

The authors declare no conflicts of interest.

**Funding:**

Iowa State University of Science and Technology Healthy Iowa Interdisciplinary Research Team Initiative

**References**

1. Meiser-Stedman R, McKinnon A, Dixon C, Boyle A, Smith P, Dalgleish T. Acute stress disorder and the transition to posttraumatic stress disorder in children and adolescents: Prevalence, course, prognosis, diagnostic suitability, and risk markers. *Depress Anxiety*. 2017;34(4). doi:10.1002/da.22602

2. Geoffrion S, Goncalves J, Robichaud I, et al. Systematic Review and Meta-Analysis on Acute Stress Disorder: Rates Following Different Types of Traumatic Events. *Trauma Violence Abuse*. 2022;23(1). doi:10.1177/1524838020933844

3. Zen AL, Whooley MA, Zhao S, Cohen BE. Post-traumatic stress disorder is associated with poor health behaviors: Findings from the Heart and Soul Study. *Health Psychology*. 2012;31(2):194-201. doi:10.1037/a0025989

4. de Assis MA, de Mello MF, Scorza FA, et al. Evaluation of Physical Activity Habits in Patients with Posttraumatic Stress Disorder. *Clinics*. 2008;63(4):473-478. doi:10.1590/S1807-59322008000400010

5. Fleshner M, Greenwood BN, Yirmiya R. Neuronal-Glial Mechanisms of Exercise-Evoked Stress Robustness. In: ; 2014:1-12. doi:10.1007/7854_2014_277

6. Nowacka-Chmielewska M, Grabowska K, Grabowski M, Meybohm P, Burek M, Małecki A. Running from Stress: Neurobiological Mechanisms of Exercise-Induced Stress Resilience. *Int J Mol Sci*. 2022;23(21):13348. doi:10.3390/ijms232113348

7. Buhr TJ, Reed CH, Wee OM, et al. The persistence of stress-induced physical inactivity in rats: an investigation of central monoamine neurotransmitters and skeletal muscle oxidative stress. *Front Behav Neurosci*. 2023;17. doi:10.3389/fnbeh.2023.1169151

8. Moraska A, Fleshner M. Voluntary physical activity prevents stress-induced behavioral depression and anti-KLH antibody suppression. *American Journal of Physiology-Regulatory, Integrative and Comparative Physiology*. 2001;281(2):R484-R489. doi:10.1152/ajpregu.2001.281.2.R484

9. Kagan J, Berkun M. The reward value of running activity. *J Comp Physiol Psychol*. 1954;47(2):108-108. doi:10.1037/h0058877

10. Iversen IH. TECHNIQUES FOR ESTABLISHING SCHEDULES WITH WHEEL RUNNING AS REINFORCEMENT IN RATS. *J Exp Anal Behav*. 1993;60(1):219-238. doi:10.1901/jeab.1993.60-219

11. Collier G, Hirsch E. Reinforcing properties of spontaneous activity in the rat. *J Comp Physiol Psychol*. 1971;77(1):155-160. doi:10.1037/h0031588

12. Belke TW. RUNNING AND RESPONDING REINFORCED BY THE OPPORTUNITY TO RUN: EFFECT OF REINFORCER DURATION. *J Exp Anal Behav*. 1997;67(3):337-351. doi:10.1901/jeab.1997.67-337

13. Rhodes JS, Garland T, Gammie SC. Patterns of Brain Activity Associated With Variation in Voluntary Wheel-Running Behavior. *Behavioral Neuroscience*. 2003;117(6):1243-1256. doi:10.1037/0735-7044.117.6.1243

14. Durieux PF, Schiffmann SN, de Kerchove d'Exaerde A. Differential regulation of motor control and response to dopaminergic drugs by D1R and D2R neurons in distinct dorsal striatum subregions. *EMBO J*. 2012;31(3):640-653. doi:10.1038/emboj.2011.400

15. Durieux PF, Bearzatto B, Guiducci S, et al. D2R striatopallidal neurons inhibit both locomotor and drug reward processes. *Nat Neurosci*. 2009;12(4):393-395. doi:10.1038/nn.2286

16. Bateup HS, Santini E, Shen W, et al. Distinct subclasses of medium spiny neurons differentially regulate striatal motor behaviors. *Proceedings of the National Academy of Sciences*. 2010;107(33):14845-14850. doi:10.1073/pnas.1009874107

17. Cox J, Witten IB. Striatal circuits for reward learning and decision-making. *Nat Rev Neurosci*. 2019;20(8):482-494. doi:10.1038/s41583-019-0189-2

18. Balleine BW, Delgado MR, Hikosaka O. The Role of the Dorsal Striatum in Reward and Decision-Making: Figure 1. *The Journal of Neuroscience*. 2007;27(31):8161-8165. doi:10.1523/JNEUROSCI.1554-07.2007

19. Saul MC, Majdak P, Perez S, Reilly M, Garland T, Rhodes JS. High motivation for exercise is associated with altered chromatin regulators of monoamine receptor gene expression in the striatum of selectively bred mice. *Genes Brain Behav*. 2017;16(3):328-341. doi:10.1111/gbb.12347

20. Rodrigues D, Jacinto L, Falcão M, et al. Chronic stress causes striatal disinhibition mediated by SOM-interneurons in male mice. *Nat Commun*. 2022;13(1):7355. doi:10.1038/s41467-022-35028-4

21. Robinson OJ, Overstreet C, Charney DR, Vytal K, Grillon C. Stress increases aversive prediction error signal in the ventral striatum. *Proceedings of the National Academy of Sciences*. 2013;110(10):4129-4133. doi:10.1073/pnas.1213923110

22. Clark PJ, Amat J, McConnell SO, et al. Running Reduces Uncontrollable Stress-Evoked Serotonin and Potentiates Stress-Evoked Dopamine Concentrations in the Rat Dorsal Striatum. *PLoS One*. 2015;10(11):e0141898. doi:10.1371/journal.pone.0141898

23. Cheng Y, Pardo M, Armini R de S, et al. Stress-induced neuroinflammation is mediated by GSK3-dependent TLR4 signaling that promotes susceptibility to depression-like behavior. *Brain Behav Immun*. 2016;53:207-222. doi:10.1016/j.bbi.2015.12.012

24. Weber MD, Frank MG, Tracey KJ, Watkins LR, Maier SF. Stress induces the danger-associated molecular pattern HMGB-1 in the hippocampus of male sprague dawley rats: A priming stimulus of microglia and the NLRP3 inflammasome. *Journal of Neuroscience*. 2015;35(1):316-324. doi:10.1523/JNEUROSCI.3561-14.2015

25. Frank MG, Baratta M V., Sprunger DB, Watkins LR, Maier SF. Microglia serve as a neuroimmune substrate for stress-induced potentiation of CNS pro-inflammatory cytokine responses. *Brain Behav Immun*. 2007;21(1):47-59. doi:10.1016/j.bbi.2006.03.005

26. Niraula A, Sheridan JF, Godbout JP. Microglia Priming with Aging and Stress. *Neuropsychopharmacology*. 2017;42(1):318-333. doi:10.1038/npp.2016.185

27. Frank MG, Weber MD, Watkins LR, Maier SF. Stress-induced neuroinflammatory priming: A liability factor in the etiology of psychiatric disorders. *Neurobiol Stress*. 2016;4:62-70. doi:10.1016/j.ynstr.2015.12.004

28. Frank MG, Fonken LK, Watkins LR, Maier SF. Acute stress induces chronic neuroinflammatory, microglial and behavioral priming: A role for potentiated NLRP3 inflammasome activation. *Brain Behav Immun*. 2020;89. doi:10.1016/j.bbi.2020.05.063

29. Fonken LK, Weber MD, Daut RA, et al. Stress-induced neuroinflammatory priming is time of day dependent. *Psychoneuroendocrinology*. 2016;66:82-90. doi:10.1016/j.psyneuen.2016.01.006

30. Fonken LK, Frank MG, Gaudet AD, Maier SF. Stress and aging act through common mechanisms to elicit neuroinflammatory priming. *Brain Behav Immun*. 2018;73:133-148. doi:10.1016/j.bbi.2018.07.012

31. Frank MG, Fonken LK, Watkins LR, Maier SF. Microglia: Neuroimmune-sensors of stress. *Semin Cell Dev Biol*. 2019;94:176-185. doi:10.1016/j.semcdb.2019.01.001

32. Marinelli S, Basilico B, Marrone MC, Ragozzino D. Microglia-neuron crosstalk: Signaling mechanism and control of synaptic transmission. *Semin Cell Dev Biol*. 2019;94:138-151. doi:10.1016/j.semcdb.2019.05.017

33. Badimon A, Strasburger HJ, Ayata P, et al. Negative feedback control of neuronal activity by microglia. *Nature*. 2020;586(7829):417-423. doi:10.1038/s41586-020-2777-8

34. Kohman RA, Bhattacharya TK, Wojcik E, Rhodes JS. Exercise reduces activation of microglia isolated from hippocampus and brain of aged mice. *J Neuroinflammation*. 2013;10(1):885. doi:10.1186/1742-2094-10-114

35. Mee-inta, Zhao, Kuo. Physical Exercise Inhibits Inflammation and Microglial Activation. *Cells*. 2019;8(7):691. doi:10.3390/cells8070691

36. Olah M, Ping G, De Haas AH, et al. Enhanced hippocampal neurogenesis in the absence of microglia T cell interaction and microglia activation in the murine running wheel model. *Glia*. 2009;57(10):1046-1061. doi:10.1002/glia.20828

37. Pervaiz N, Hoffman-Goetz L. Immune cell inflammatory cytokine responses differ between central and systemic compartments in response to acute exercise in mice. *Exerc Immunol Rev*. 2012;18:142-157. http://www.ncbi.nlm.nih.gov/pubmed/22876726

38. Ehninger D. Regional Effects of Wheel Running and Environmental Enrichment on Cell Genesis and Microglia Proliferation in the Adult Murine Neocortex. *Cerebral Cortex*. 2003;13(8):845-851. doi:10.1093/cercor/13.8.845

39. He X fei, Liu D xu, Zhang Q, et al. Voluntary Exercise Promotes Glymphatic Clearance of Amyloid Beta and Reduces the Activation of Astrocytes and Microglia in Aged Mice. *Front Mol Neurosci*. 2017;10. doi:10.3389/fnmol.2017.00144

40. Kohman RA, DeYoung EK, Bhattacharya TK, Peterson LN, Rhodes JS. Wheel running attenuates microglia proliferation and increases expression of a proneurogenic phenotype in the hippocampus of aged mice. *Brain Behav Immun*. 2012;26(5):803-810. doi:10.1016/j.bbi.2011.10.006

41. Vukovic J, Colditz MJ, Blackmore DG, Ruitenberg MJ, Bartlett PF. Microglia Modulate Hippocampal Neural Precursor Activity in Response to Exercise and Aging. *The Journal of Neuroscience*. 2012;32(19):6435-6443. doi:10.1523/JNEUROSCI.5925-11.2012

42. Wang J, Yue B, Zhang X, Guo X, Sun Z, Niu R. Effect of exercise on microglial activation and transcriptome of hippocampus in fluorosis mice. *Science of The Total Environment*. 2021;760:143376. doi:10.1016/j.scitotenv.2020.143376

43. Gerecke KM, Kolobova A, Allen S, Fawer JL. Exercise protects against chronic restraint stress-induced oxidative stress in the cortex and hippocampus. *Brain Res*. 2013;1509:66-78. doi:10.1016/j.brainres.2013.02.027

44. Xiao K, Luo Y, Liang X, et al. Beneficial effects of running exercise on hippocampal microglia and neuroinflammation in chronic unpredictable stress-induced depression model rats. *Transl Psychiatry*. 2021;11(1):461. doi:10.1038/s41398-021-01571-9

45. Zhang J, Rong P, Zhang L, et al. IL4-driven microglia modulate stress resilience through BDNF-dependent neurogenesis. *Sci Adv*. 2021;7(12). doi:10.1126/sciadv.abb9888

46. Reed CH, Bauer EE, Shoeman A, Buhr TJ, Clark PJ. Acute Stress Exposure Alters Food-Related Brain Monoaminergic Profiles in a Rat Model of Anorexia. *J Nutr*. 2021;151(12):3617-3627. doi:10.1093/jn/nxab298

47. Clark PJ, Ghasem PR, Mika A, et al. Wheel running alters patterns of uncontrollable stress-induced cfos mRNA expression in rat dorsal striatum direct and indirect pathways: A possible role for plasticity in adenosine receptors. *Behavioural Brain Research*. 2014;272:252-263. doi:10.1016/j.bbr.2014.07.006

48. Strong PV, Christianson JP, Loughridge AB, et al. 5-hydroxytryptamine 2C receptors in the dorsal striatum mediate stress-induced interference with negatively reinforced instrumental escape behavior. *Neuroscience*. 2011;197:132-144. doi:10.1016/j.neuroscience.2011.09.041

49. Greenwood BN, Foley TE, Burhans D, Maier SF, Fleshner M. The consequences of uncontrollable stress are sensitive to duration of prior wheel running. *Brain Res*. 2005;1033(2):164-178. doi:10.1016/j.brainres.2004.11.037

50. Greenwood BN, Foley TE, Day HEW, et al. Freewheel Running Prevents Learned Helplessness/Behavioral Depression: Role of Dorsal Raphe Serotonergic Neurons. *The Journal of Neuroscience*. 2003;23(7):2889-2898. doi:10.1523/JNEUROSCI.23-07-02889.2003

51. Bauer EE, Shoeman A, Buhr TJ, Daniels KM, Lyte M, Clark PJ. Voluntary binge□patterned alcohol drinking and sex□specific influences on monoamine□related neurochemical signatures in the mouse gut and brain. *Alcohol Clin Exp Res*. 2021;45(5):996-1012. doi:10.1111/acer.14592

52. Buhr TJ, Reed CH, Shoeman A, Bauer EE, Valentine RJ, Clark PJ. The Influence of Moderate Physical Activity on Brain Monoaminergic Responses to Binge-Patterned Alcohol Ingestion in Female Mice. *Front Behav Neurosci*. 2021;15. doi:10.3389/fnbeh.2021.639790

53. Johnson Z V., Hegarty BE, Gruenhagen GW, Lancaster TJ, McGrath PT, Streelman JT. Cellular profiling of a recently-evolved social behavior in cichlid fishes. *Nat Commun*. 2023;14(1):4891. doi:10.1038/s41467-023-40331-9

54. Heaton H, Talman AM, Knights A, et al. Souporcell: robust clustering of single-cell RNA-seq data by genotype without reference genotypes. *Nat Methods*. 2020;17(6):615-620. doi:10.1038/s41592-020-0820-1

55. Hao Y, Hao S, Andersen-Nissen E, et al. Integrated analysis of multimodal single-cell data. *Cell*. 2021;184(13):3573-3587.e29. doi:10.1016/j.cell.2021.04.048

56. Bai Y, Chu L. A Graph-based Approach to Estimating the Number of Clusters. *arXiv preprint*. 2024;arXiv:2402.15600.

57. Tibshirani R, Walther G, Hastie T. Estimating the Number of Clusters in a Data Set Via the Gap Statistic. *J R Stat Soc Series B Stat Methodol*. 2001;63(2):411-423. doi:10.1111/1467-9868.00293

58. Ahlmann-Eltze C, Huber W. glmGamPoi: fitting Gamma-Poisson generalized linear models on single cell count data. *Bioinformatics*. 2021;36(24):5701-5702. doi:10.1093/bioinformatics/btaa1009

59. Storey JD, Tibshirani R. Statistical significance for genomewide studies. *Proceedings of the National Academy of Sciences*. 2003;100(16):9440-9445. doi:10.1073/pnas.1530509100

60. Wu T, Hu E, Xu S, et al. clusterProfiler 4.0: A universal enrichment tool for interpreting omics data. *Innovation*. 2021;2(3). doi:10.1016/j.xinn.2021.100141

61. Yu G, Wang LG, Han Y, He QY. clusterProfiler: an R Package for Comparing Biological Themes Among Gene Clusters. *OMICS*. 2012;16(5):284-287. doi:10.1089/omi.2011.0118

62. Gulati GS, Sikandar SS, Wesche DJ, et al. Single-cell transcriptional diversity is a hallmark of developmental potential. *Science (1979)*. 2020;367(6476):405-411. doi:10.1126/science.aax0249

63. Fediuc S, Campbell JE, Riddell MC. Effect of voluntary wheel running on circadian corticosterone release and on HPA axis responsiveness to restraint stress in Sprague-Dawley rats. *J Appl Physiol*. 2006;100(6):1867-1875. doi:10.1152/japplphysiol.01416.2005

64. Droste SK, Chandramohan Y, Hill LE, Linthorst ACE, Reul JMHM. Voluntary Exercise Impacts on the Rat Hypothalamic-Pituitary-Adrenocortical Axis Mainly at the Adrenal Level. *Neuroendocrinology*. 2007;86(1):26-37. doi:10.1159/000104770

65. Lee JR, Parker KE, Tapia M, et al. Voluntary wheel running effects on intra-accumbens opioid high-fat feeding and locomotor behavior in Sprague-Dawley and Wistar rat strains. *Physiol Behav*. 2019;206:67-75. doi:10.1016/j.physbeh.2019.02.015

66. Thrupp N, Sala Frigerio C, Wolfs L, et al. Single-Nucleus RNA-Seq Is Not Suitable for Detection of Microglial Activation Genes in Humans. *Cell Rep*. 2020;32(13):108189. doi:10.1016/j.celrep.2020.108189

67. Mathys H, Davila-Velderrain J, Peng Z, et al. Single-cell transcriptomic analysis of Alzheimer's disease. *Nature*. 2019;570(7761):332-337. doi:10.1038/s41586-019-1195-2

68. Wahane S, Zhou X, Zhou X, et al. Diversified transcriptional responses of myeloid and glial cells in spinal cord injury shaped by HDAC3 activity. *Sci Adv*. 2021;7(9). doi:10.1126/sciadv.abd8811

69. Hammond TR, Dufort C, Dissing-Olesen L, et al. Single-Cell RNA Sequencing of Microglia throughout the Mouse Lifespan and in the Injured Brain Reveals Complex Cell-State Changes. *Immunity*. 2019;50(1):253-271.e6. doi:10.1016/j.immuni.2018.11.004

70. Schafer DP, Lehrman EK, Kautzman AG, et al. Microglia Sculpt Postnatal Neural Circuits in an Activity and Complement-Dependent Manner. *Neuron*. 2012;74(4):691-705. doi:10.1016/j.neuron.2012.03.026

71. Stevens B, Allen NJ, Vazquez LE, et al. The Classical Complement Cascade Mediates CNS Synapse Elimination. *Cell*. 2007;131(6):1164-1178. doi:10.1016/j.cell.2007.10.036

72. Ruan Z, Cao G, Qian Y, et al. Single-cell RNA sequencing unveils Lrg1's role in cerebral ischemia reperfusion injury by modulating various cells. *J Neuroinflammation*. 2023;20(1):285. doi:10.1186/s12974-023-02941-4

73. Bayne K. Environmental enrichment and mouse models: Current perspectives. *Animal Model Exp Med*. 2018;1(2):82-90. doi:10.1002/ame2.12015

74. Nithianantharajah J, Hannan AJ. Enriched environments, experience-dependent plasticity and disorders of the nervous system. *Nat Rev Neurosci*. 2006;7(9):697-709. doi:10.1038/nrn1970

75. Clemenson GD, Deng W, Gage FH. Environmental enrichment and neurogenesis: from mice to humans. *Curr Opin Behav Sci*. 2015;4:56-62. doi:10.1016/j.cobeha.2015.02.005

76. Zhou Y, Song WM, Andhey PS, et al. Human and mouse single-nucleus transcriptomics reveal TREM2-dependent and TREM2-independent cellular responses in Alzheimer's disease. *Nat Med*. 2020;26(1):131-142. doi:10.1038/s41591-019-0695-9

77. Li Q, Cheng Z, Zhou L, et al. Developmental Heterogeneity of Microglia and Brain Myeloid Cells Revealed by Deep Single-Cell RNA Sequencing. *Neuron*. 2019;101(2):207-223.e10. doi:10.1016/j.neuron.2018.12.006

78. Blandino P, Barnum CJ, Deak T. The involvement of norepinephrine and microglia in hypothalamic and splenic IL-1β responses to stress. *J Neuroimmunol*. 2006;173(1-2):87-95. doi:10.1016/j.jneuroim.2005.11.021

79. Grégoire CA, Bonenfant D, Le Nguyen A, Aumont A, Fernandes KJL. Untangling the Influences of Voluntary Running, Environmental Complexity, Social Housing and Stress on Adult Hippocampal Neurogenesis. *PLoS One*. 2014;9(1):e86237. doi:10.1371/journal.pone.0086237

80. Mustroph ML, Chen S, Desai SC, Cay EB, DeYoung EK, Rhodes JS. Aerobic exercise is the critical variable in an enriched environment that increases hippocampal neurogenesis and water maze learning in male C57BL/6J mice. *Neuroscience*. 2012;219:62-71. doi:10.1016/j.neuroscience.2012.06.007

81. Kobilo T, Liu QR, Gandhi K, Mughal M, Shaham Y, van Praag H. Running is the neurogenic and neurotrophic stimulus in environmental enrichment. *Learning & Memory*. 2011;18(9):605-609. doi:10.1101/lm.2283011

82. Lehrman EK, Wilton DK, Litvina EY, et al. CD47 Protects Synapses from Excess Microglia-Mediated Pruning during Development. *Neuron*. 2018;100(1):120-134.e6. doi:10.1016/j.neuron.2018.09.017

83. Scott□Hewitt N, Perrucci F, Morini R, et al. Local externalization of phosphatidylserine mediates developmental synaptic pruning by microglia. *EMBO J*. 2020;39(16). doi:10.15252/embj.2020105380

84. Paolicelli RC, Bolasco G, Pagani F, et al. Synaptic pruning by microglia is necessary for normal brain development. *Science (1979)*. 2011;333(6048):1456-1458. doi:10.1126/science.1202529

85. Kim HJ, Cho MH, Shim WH, et al. Deficient autophagy in microglia impairs synaptic pruning and causes social behavioral defects. *Mol Psychiatry*. 2017;22(11):1576-1584. doi:10.1038/mp.2016.103

86. Morgan BP, Kavanagh D. Introduction to complement in health and disease: novel aspects and insights. *Semin Immunopathol*. 2018;40(1):1-2. doi:10.1007/s00281-017-0664-7

87. Reis ES, Mastellos DC, Hajishengallis G, Lambris JD. New insights into the immune functions of complement. *Nat Rev Immunol*. 2019;19(8):503-516. doi:10.1038/s41577-019-0168-x

88. Soto I, Graham LC, Richter HJ, et al. APOE Stabilization by Exercise Prevents Aging Neurovascular Dysfunction and Complement Induction. *PLoS Biol*. 2015;13(10):e1002279. doi:10.1371/journal.pbio.1002279

89. Li F, Geng X, Yun HJ, Haddad Y, Chen Y, Ding Y. Neuroplastic Effect of Exercise Through Astrocytes Activation and Cellular Crosstalk. *Aging Dis*. 2021;12(7):1644. doi:10.14336/AD.2021.0325